JOURNAL OF CATALYSIS **172,** 137–145 (1997)
ARTICLE NO. CA971848

Effect of Alumina Fluoridation on Hydroconversion of *n*-Heptane on Sulfided NiW/Al_2O_3 Catalysts

A. Benitez,*[,1] J. Ramirez,† J. Cruz-Reyes,*[,2] and A. López Agudo*[,3]

*Instituto de Catálisis y Petroleoquímica, CSIC, Campus UAM, Cantoblanco, Madrid 28049, Spain; and †Facultad de Química, UNAM, Ciudad Universitaria, México D.F. 04510, México

Received March 25, 1997; revised June 23, 1997; accepted July 24, 1997

Hydroisomerization and hydrocracking of *n*-heptane on sulfided NiW catalysts, supported on alumina modified with various amounts of fluoride, have been studied at 673, 698, and 723 K and at a total pressure of 3 MPa. It was found that alumina fluoridation increases the catalytic activity for both hydroisomerization and hydrocracking and provides a higher hydroisomerization selectivity. Differences in product selectivities for the hydroisomerization and hydrocracking of *n*-heptane indicate that alumina fluoridation induces also changes in the various contributions of the mechanisms involved in the transformation of *n*-heptane. A decrease in the ratio of 3-MC_6 and 2-MC_6 monobranched isomers predicted by a branching mechanism via the protonated cyclopropane (PCP) intermediates and a decrease in the dimerization cracking mechanism in favor of the classic bifunctional cracking mechanism were observed with increasing fluoride content. Theses changes are results of a better balance of the (de)hydrogenation and acidity functions of the sulfided catalysts with increasing fluoride content since the incorporation of fluoride increases the (de)hydrogenation function and decreases the strength of the acid sites. © 1997 Academic Press

INTRODUCTION

The process known as mild hydrocracking is a relatively modern hydrocracking process oriented to the production of low-sulfur fuel oil and middle distillates which are in increasing demand (1, 2). This type of process is operated at lower H_2 pressure than conventional hydrocracking and at temperatures slightly higher than hydrotreating. It is considered to be an evolution of the gas oil hydrodesulfurization process. Since the present feedstocks to be treated contain significant amounts of heteroatom (S, N, O) containing molecules, the catalysts for this hydrocracking process must have good cracking activity and must also be able to catalyze S and N removal. Therefore, the conventional nonacid hydrotreating catalysts of metal sulfides on alumina are generally changed for slightly more acidic catalysts consisting of mixed Ni–Mo or Ni–W sulfides on more acidic supports, usually zeolite, silica-alumina or alumina modified with boron, halogens, or phosphorus. However, relatively few studies have been reported in the literature on these metal sulfide-based mild hydrocracking catalysts (3–9).

An earlier paper reported results of the optimization of hydrocracking catalysts for maximum production of middle distillates (3); different couples of mixed metal sulfides and compositions of silica-alumina supports were studied in order to obtain a balanced catalyst offering the best selectivity toward middle distillates and the highest possible activity. For zeolite-supported metal sulfide catalysts, several studies have been reported on hydrocracking of *n*-heptane (4–7) and long-chain alkanes, like *n*-decane (8, 9). In general, these studies showed that such catalysts have generally good activity but quite different product selectivities from those found with Pt or Pd on zeolite due to the weaker hydrogenation activity of the metal sulfides. Thus, Ni–Mo/ultrastable HY catalysts for hydrocracking of *n*-heptane were shown to present an intermediate behavior between that of an ideal bifunctional Pt/HY zeolite catalyst and that of a monofunctional ultrastable HY zeolite cracking catalyst with respect to product selectivity (4). A similar behavior was also found for sulfided NiMo/HY zeolite catalysts (6), where the relative strength of the hydrogenation–dehydrogenation function and the acidity determines activity and product selectivity. On the widely used industrial Ni–W hydrotreating catalysts supported on alumina or acidic modified alumina, there is still a lack of fundamental understanding about the roles of the catalytic dual functionality in hydrocracking reactions. Concerning hydroprocessing over NiW catalysts supported on fluoride-modified alumina, only a preliminary study of thiophene hydrodesulfurization and *n*-heptane hydrocracking has been reported (10).

The aim of the present work is to investigate the effect of the incorporation of different amounts of fluoride

[1] Present address: Facultad de Química, UNAM, Ciudad Universitaria, México D.F. (04510), México.
[2] Present address: Facultad de Ciencias Químicas, UABC, Apartado Postal 117-B, Tijuana, BC 2100, México.
[3] Corresponding author. Fax: (+34-1)5854760.

0021-9517/97 $25.00
Copyright © 1997 by Academic Press
All rights of reproduction in any form reserved.

to the alumina support on activity and selectivity of NiW/Al_2O_3–F(x) catalysts for the hydroisomerization and hydrocracking of *n*-heptane. This compound is one of the model molecules most frequently chosen for hydrocracking studies because is the simplest *n*-alkane which allows to evaluate adequately the isomerization/cracking selectivity of bifunctional catalysts.

EXPERIMENTAL

Catalyst Preparation

The NiW/Al_2O_3 catalysts used in the present study were same as those described in a previous work on hydrotreating (11). They were prepared by conventional pore volume co-impregnation of the W (ammonium metatungstate) and Ni (nickel nitrate) precursors on γ-alumina preimpregnated with different amounts of NH_4F. The samples were dried at 383 K for 2 h, then calcined at 653 K for 2.5 h and finally at 823 K for 4.5 h. The metal loadings were 20.9 wt% WO_3 and 3.17 wt% NiO, and the fluoride content in the alumina varied in the range 0–2.5 wt% F^-. Catalyst samples are denoted as NiW–F(x), with x representing the wt% F^-.

Apparatus and Procedure

Hydroconversion of *n*-heptane was measured in a conventional high pressure stainless steel continuous flow microreactor. Catalyst particles of 1.19–0.84 mm were diluted 1 : 1 with SiC of similar particle size and loaded in the reactor. Particles of SiC were placed in the top and bottom parts of the reactor to obtain an evenly distributed flow of reactants. Before reaction the catalysts were presulfided using a mixture of H_2S/H_2 (10% vol H_2S) at atmospheric pressure and 623 K for 4 h. After catalyst sulfiding the preheater and reactor were slowly heated up to the desired temperature under a flow of H_2. After the reaction temperature was reached, the H_2 flow and pressure were then adjusted to the experimental value, and the hydrocarbon was fed at the desired rate. The reaction was then studied under the following conditions: weight of catalysts, 50 mg; temperature, 673, 698, 723 K; total pressure, 3 MPa; molar ratio of H_2/*n*-heptane, 5; and liquid flow rate was varied (12–30 $cm^3\ h^{-1}$) to obtain different values of the space time W/F (weight of catalyst/molar flow rate of *n*-heptane) in the range 2.5–6.28 $g \cdot h \cdot mol^{-1}$.

A stabilization time of 90 min was maintained before each experiment. After removal of the stabilization period liquid products, the test run was started. The liquid product accumulated during 60 or 120 min (depending on the flow rate used) was collected from the high pressure receiver, weighted, and analyzed. During each test run, at regular periods the gaseous products were measured and withdrawn for analysis. The total gas volume passed at the end of each test period was also recorded. Usually a series of two test runs were made at the same conditions to test the reproducibility of the data. Since in preliminary experiments these catalysts showed no significant deactivation under the conditions used, all the runs at different reaction temperature and space time were generally carried out on the same charge of catalyst. Moreover, catalyst stability was also controlled by conducting a reference experiment at different time during the catalyst testing. Between experiments the catalyst was kept under H_2 pressure (>0.5 MPa) at room temperature.

The analysis of the liquid products was carried out with a gas chromatograph equipped with a 50-m methyl silicone column (HP-1, ID 0.31 mm, film thickness 0.52 μm) using temperature programming (313 K for 12 min, followed by an increase up to 343 K at a rate of 10 K/min) and a He flow of 1 $cm^3\ min^{-1}$, with flame ionization detection. The gaseous products were analyzed in two columns: (1) capillary column with the same specifications as for the liquid products analysis; (2) a 3-m × 1/8″ column packed with Carbosieve S II, using temperature programming (308 K for 7 min, followed by heating up to 498 K at a 10 K/min rate and held at 498 K for 14 min) and a He flow of 10 $cm^3\ min^{-1}$, and TC detector. The Carbosieve S II column allowed the separation and detection of H_2 and light hydrocarbons, while the capillary column allowed the analysis of small amounts of heavier liquid products in the gas phase. Product identification was based in the retention time of the pure compounds.

The course of the reaction was described by three conversions. The overall conversion of *n*-heptane, x_T, defined as the number of *n*-heptane moles converted to products divided by the number of *n*-heptane moles in the feed, calculated on the basis of number of carbon atoms in products and *n*-heptane. Possible *n*-heptane converted to coke was not included. The conversion of *n*-heptane to C_7-isomers, x_I, given by the sum of moles of C_7-isomers produced divided by the number of *n*-heptane moles in the feed. Similarly, the conversion of *n*-heptane to cracking products, x_{HC}, defined as the ratio of moles of cracked products/*n*-heptane moles fed. Product selectivity, S_I, is expressed as moles of a given product per 100 moles of *n*-heptane reacted, also on the basis of number of carbon atoms.

RESULTS

Activity and Selectivity in n-Heptane Hydroconversion

Under the experimental conditions used in this study, the reaction products consisted almost entirely of skeletally isomerized heptane (2-methylhexane (2-MC_6) and 3-methylhexane (3-MC_6)), and hydrocracked products. Table 1 shows typical product distributions and selectivities obtained at 698 K with the two more representative catalysts, NiW–F(0) and NiW–F(2.5), at different levels of conversion. It is observed that the hydrocracked products were

TABLE 1

Hydroconversion of *n*-Heptane at 698 K on NiW–(F0) and NiW–F(2.5) Catalysts

Catalyst	NiW–F(0)				NiW–F(2.5)				
Total conversion (%)	0.63	0.92	1.03	1.15	9.4	11.5	13.7	16.6	18.5
Hydroisomerization	0.30	0.40	0.51	0.70	8.4	10.2	11.9	14.7	16.3
Hydrocracking	0.33	0.52	0.52	0.45	1.1	1.3	1.7	1.9	2.2
Product selectivity (distribution of hydroisomerized and hydrocracked fractions) (%)									
2-MC_6	19.5 (40.0)	17.5 (40)	18.9 (39.1)	24.1 (39.0)	42.1 (47.5)	42.3 (47.5)	41.6 (47.5)	42.4 (47.9)	40.4 (46.0)
3-MC_6	28.7 (60.0)	26.3 (60)	29.4 (60.9)	37.1 (61.0)	46.5 (52.5)	46.7 (52.5)	45.9 (52.4)	46.1 (52.1)	47.5 (54.0)
C_1	—	—	—	1.2 (4.4)	—	—	—	<0.1 (0.1)	<0.1 (0.1)
C_2	—	—	—	—	—	—	—	—	—
C_3	21.7 (40)	22.3 (39.8)	18.5 (34.3)	8.3 (21.1)	4.2 (37.2)	3.8 (35.3)	4.7 (37.8)	4.2 (36.9)	4.2 (35.1)
i-C_4	0.9 (3.1)	1.0 (1.9)	0.9 (1.9)	0.3 (0.5)	1.1 (8.8)	1.0 (8.7)	1.1 (9.1)	1.2 (10.3)	1.3 (10.3)
n-C_4	19.1 (39.4)	19.5 (34.9)	18.3 (36.2)	13.5 (34.4)	3.5 (31.2)	3.4 (30.9)	3.8 (30.5)	3.2 (28.8)	3.6 (29.5)
i-C_5	—	—	—	0.1 (0.5)	0.5 (4.3)	0.5 (4.7)	0.6 (4.4)	0.5 (4.7)	0.6 (5.2)
n-C_5	9.7 (18.5)	8.9 (15.5)	9.4 (18.1)	9.5 (24.5)	1.4 (12.1)	1.4 (13.1)	1.5 (12.0)	1.3 (11.9)	1.5 (12.1)
n-C_6	0.4 (0.1)	4.3 (7.8)	4.6 (9.5)	5.8 (15.6)	0.7 (6.5)	0.8 (7.1)	0.7 (5.8)	0.7 (6.4)	0.8 (6.7)

Note. Product selectivities (%) and internal distribution of hydroisomerized and hydrocracked fractions (%, within brackets).

mainly composed of propane, iso- and *n*-butane, iso- and *n*-pentane, and hexane, accompanied by very small amounts of methane, ethane and 2- and 3-methylpentane. The latter cracked products, and particularly the C_1 and C_2, were generally observed at high conversions and temperatures; however, their yield was below 0.15% or as traces. In some cases, the formation of very small amounts of dehydrocyclization products (methylcyclohexane and toluene) were also detected but at concentration <0.01%. Thus, hydroconversion of *n*-heptane on these catalysts consists essentially of two main reactions: hydroisomerization and hydrocracking.

To see whether hydrocracking occurred consecutively or simultaneously to the hydroisomerization reaction, the overall initial selectivities for hydroisomerization and hydrocracking were calculated by extrapolating the hydroisomerization and hydrocracking product selectivity versus total conversion curves to zero conversion. The initial selectivity values revealed that isomerization and cracking products appear as primary products of the reaction for all the catalysts and are formed at a different rate. Figure 1 shows the effect of fluoride on the initial selectivity of the reaction for overall hydroisomerization and hydrocracking products. A gradual increase in hydroisomerization and a decrease in hydrocracking is observed when the fluoride content in the catalysts is increased up to about 1.5 wt%; above such a value the selectivity is almost constant. It is remarkable that the hydroisomerization selectivity is nearly doubled with fluoride contents above 1.5 wt%. Thus, at 698 K the initial selectivities for both hydroisomerization and hydrocracking were close to 50% for the fluoride-free catalyst, whereas over the NiW–F(2.5) catalyst they were 90 and 10% for hydroisomerization and hydrocracking, respectively. With increasing reaction temperature the selectivity of isomerized heptane shows a slight tendency to decrease while that for the cracked heptane products shows the reverse trend, suggesting that at high temperatures somewhat hydroisomerized *n*-heptane is likely to undergo hydrocracking.

The effect of the space time (W/F) on hydroisomerization, hydrocracking, and total conversion of *n*-heptane at 698 K over the different catalysts is shown in Fig. 2. For the W/F interval studied, the overall conversion, as well as the conversions to hydroisomerization and hydrocracking increase with space time. In agreement with other studies (6, 12–14), our results were found to fit a simple first-order kinetic equation satisfactorily, as Fig. 3 shows for the hydroisomerization data. The variations of the calculated rate constants for *n*-heptane hydroisomerization (k_I) and hydrocracking (k_{HC}) at 673, 698, and 723 K are shown in

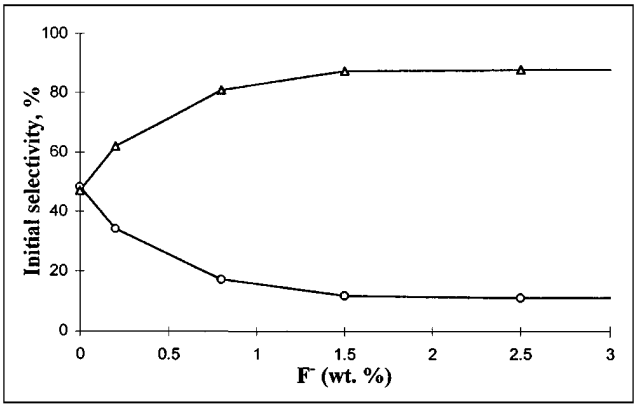

FIG. 1. Effect of fluoride content on the initial selectivity for hydroisomerization (△) and hydrocracking (○) of *n*-heptane over NiW–F(*x*) catalysts at 698 K.

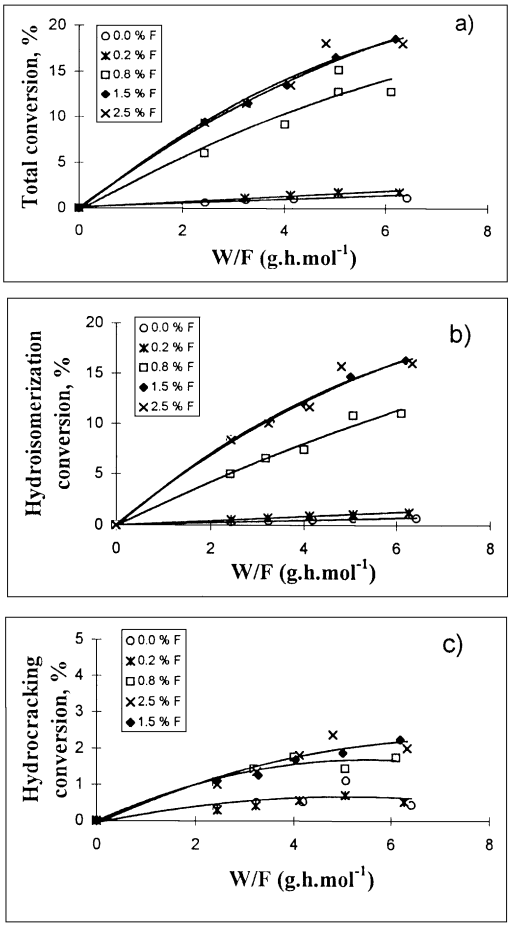

FIG. 2. Effect of space-time (W/F) on total conversion (a), hydroisomerization (b), and hydrocracking (c) of *n*-heptane on NiW–F(x) catalysts at 698 K.

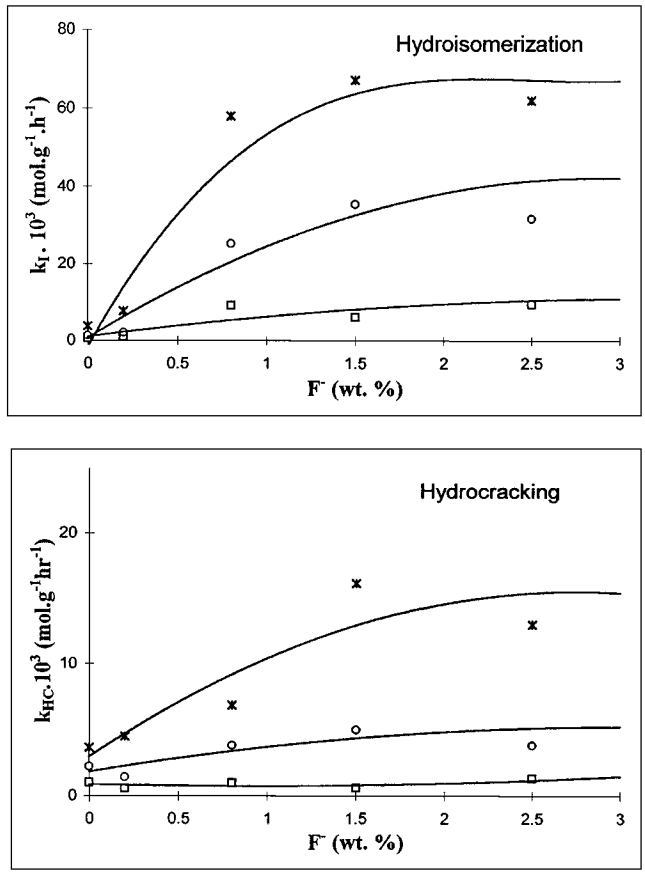

FIG. 4. Effect of fluoride content on the reaction rate constant for hydroisomerization and hydrocracking of *n*-heptane at 673 K (□); 698 K (○), and 723 K (∗). W/F = 5 g · h · mol^{-1}.

Fig. 4 as a function of the fluoride content. Figure 4 reveals that at low fluoride content, the rates of hydroisomerization and hydrocracking of *n*-heptane are little or not influenced by fluoride, but within the 0.2–1.5 wt% F^- range the reaction rate constants, especially that of hydroisomerization, are considerably increased. Further fluoride addition beyond 1.5 wt% F^- has no further effect on the rate constants. This effect of fluoride was more pronounced with increasing temperature.

The apparent activation energies for hydroisomerization and hydrocracking of *n*-heptane, obtained from the k_I and k_{HC} values of Fig. 4, are summarized in Table 2. The apparent activation energy for hydroisomerization of *n*-heptane is similar for all catalysts, while that for *n*-heptane hydrocracking seems to increase with increasing fluoride content.

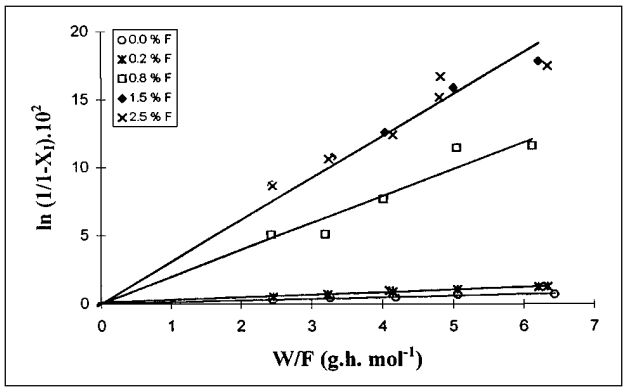

FIG. 3. First-order plot for hydroisomerization of *n*-heptane on NiW–F(x) catalysts at 698 K.

TABLE 2

Apparent Activation Energy of the Catalysts

Catalyst	Ea (Kcal/mol)	
	Hydroisomerization	Hydrocracking
NiW–F(0)	36	25
NiW–F(0.2)	38	30
NiW–F(0.8)	36	40
NiW–F(1.5)	42	48
NiW–F(2.5)	36	44

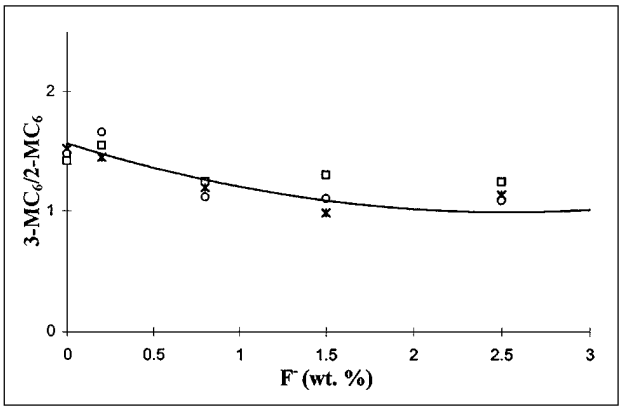

FIG. 5. Effect of fluoride content on the molar ratio of 3-MC_6/2-MC_6 in the reaction products at 673 K (□); 698 K (◯), and 723 K (∗). W/F = 5 g · h · mol^{-1}.

Distribution of the Hydroisomerized Products

The only C_7-isomers found in the reaction products were the monobranched 2-MC_6 and 3-MC_6, both appeared as primary products; no multibranched C_7-isomers were detected. For each catalyst, the ratio of the 2-MC_6 and 3-MC_6 isomers was almost independent on the total conversion, and the formation of 3-MC_6 was generally favored with respect to 2-MC_6 (Table 1). Figure 5 shows that the 3-MC_6/2-MC_6 molar ratio decreased gradually with increasing fluoride content from the initial value of 1.5 (at 698 K) for the fluoride-free catalyst to about 1.1 for the NiW–F(2.5) catalyst.

The reaction temperature hardly affected the 3-MC_6/2-MC_6 molar ratio, as shown in Fig. 5.

Distribution of the Hydrocracked Products

As shown in Tables 1 and 3, propane and butane were the main hydrocracking products accounting for more than 65–80% of the hydrocraked products. This tendency to produce large fragments is indicative of a carbenium ion mechanism in which the hydrocracking occurs preferentially at the center of the C_7 molecule. As the C_3 and C_4 products are not formed in equimolar amounts, the cracking mechanism strongly deviates from the ideal hydrocracking (15). Furthermore, pentanes and hexanes appeared as minor products but in significant amounts, while methane and ethane were measurable only in some cases. Consequently, the molar distribution of hydrocracked products was slightly asymmetric, with higher values for $C_4 + C_5 + C_6$ than for $C_3 + C_2 + C_1$, suggesting that a small part of the C_4, C_5, and C_6 fractions may not result from the primary hydrocracking or hydrogenolysis of C_7 but from secondary cracking of previous products from bimolecular condensation and alkylation reactions, as has been observed in the cracking of alkanes on zeolites (12, 13, 16–18) and also in the hydrocracking of *n*-heptane on Ni–Mo/HY ultrastable zeolite (4, 6).

Table 4 gives the initial selectivities to hydrocracked products calculated with respect to total *n*-heptane converted. The C_3, C_4, and C_5 fractions appear as primary products for all catalyst and the C_6 fraction appears as secondary on the NiW–F(0) and NiW–F(0.2) catalysts and as slightly primary on the other catalysts. The initial selectivities to cracking products apparently decrease with increasing fluoride content. However, this small effect might be the result of a change in the hydroisomerization/hydrocracking activity ratio. Since practically all hydrocracked products are apparently primary, in order to see whether fluoride content affects the distribution of hydrocracked products, the hydrocracking reaction was considered separately and the selectivities to hydrocracked products were recalculated on the basis of hydrocracked *n*-heptane only. The selectivity to C_1 and C_2 were, however, not considered because of the very limited number of data available and also the very low yields of these products. With the recalculated initial selectivities to hydrocracked products, Fig. 6 shows that the

TABLE 3

Composition (%) of the Hydrocracked Fraction from Hydroconversion of *n*-Heptane on the NiW–F(1.5) Catalyst at Different Temperatures and Conversion Levels

	673 K	698 K		723 K	
Total conversion, X_T (%)	3.22	16.07	21.13	35.22	37.03
Hydrocracking, X_{HC} (%)	0.24	1.54	3.65	7.38	9.07
C_1	—	—	—	1.2	1.5
C_2	—	—	—	—	—
C_3	25.6	23.7	46.3	41.9	40.8
i-C_4	3.2	14.6	22.2	25.5	26.3
n-C_4	43.2	30.8	20.7	20.7	20.7
i-C_5	—	7.0	3.2	4.1	3.8
n-C_5	29.6	15.9	4.8	4.0	3.5
2-MC_5	—	—	—	—	1.2
n-C_6	<0.1	8.1	2.8	2.1	1.9

TABLE 4

Initial Selectivities[a] to Hydrocracked Products in the Hydroconversion of *n*-Heptane on NiW–F(*x*) Catalysts

	Catalyst				
Product	NiW–F(0)	NiW–F(0.2)	NiW–F(0.8)	NiW–F(1.5)	NiW–F(2.5)
C_3	19.40	13.63	8.06	5.03	4.01
i-C_4	0.88	0.52	0.82	0.87	1.06
n-C_4	18.52	13.05	5.61	3.60	3.45
ΣC_4	19.89	13.77	6.51	4.47	4.52
i-C_5	0.00	0.12	0.00	0.49	0.53
n-C_5	8.93	6.64	1.98	1.39	1.46
ΣC_5	8.93	6.76	1.98	1.88	1.99
n-C_6	0.00	0.00	0.84	0.63	0.75

[a] Calculated with respect to total *n*-heptane converted.

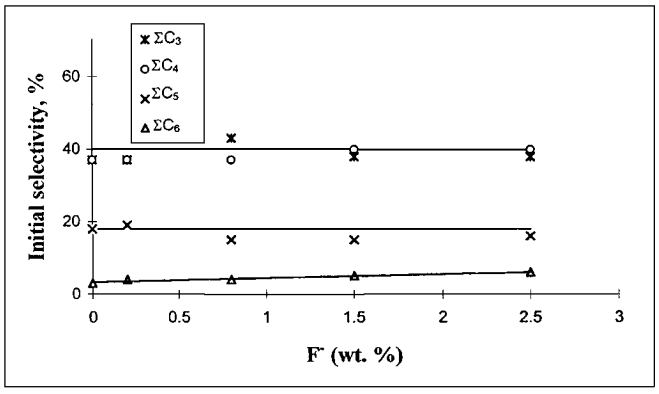

FIG. 6. Effect of fluoride content on initial selectivity to hydrocracked products over NiW–F(x) catalysts at 698 K.

fluoride content does not significantly modify the initial selectivity to C_3, C_4, and C_5 fractions, only the selectivity to C_6, which initially is very low, increases slightly with increasing fluoride content. This observation, together with the fact that C_1 appeared mainly at high conversions and only with the catalyst with the highest fluoride content, indicates that the hydrogenolysis reaction increases slightly with fluoride content.

The iso/normal molar ratios in the C_4 and C_5 fractions were generally very low for all the catalysts, increasing gradually with fluoride content up to 1.5 wt% F^- and then decreased slightly, as shown in Fig. 7. For the NiW–F(0) and NiW–F(0.2) catalysts, the i-C_4/n-C_4 ratio did not change significantly with increasing reaction temperature and the i-C_5/n-C_5 increased slightly, while for the other catalysts both i-C_4/n-C_4 and i-C_5/n-C_5 ratios clearly increased (see Fig. 7).

DISCUSSION

The results of Fig. 2 show that total conversion of n-heptane increases with the incorporation of fluoride content up to about 1.5 wt% F. It is also evident from Figs. 2–4 that both hydroisomerization and hydrocracking activities are increased with fluoride incorporation, although the increase is smaller for hydrocracking than for hydroisomerization. As a consequence, with increasing fluoride content the reaction selectivity of the NiW–F(x) catalysts changes towards higher hydroisomerization and lower hydrocracking, as shown in Fig. 1. This increase in the hydroisomerization/hydrocracking ratio could, in principle, be interpreted as due to a relative strengthening of the (de)hydrogenation function with respect to the acidity.

This proposal will be examined taking into account our previous results of characterization and hydrotreating activity on the same catalysts (11). In this study the characterization data obtained by using different methods, including XPS, DRS, and IR of adsorbed NO, showed that increasing the fluoride content decreased the Ni and W dispersion and, on the other hand, improved the sulfidation of the Ni and W phases. It could be expected that the decrease in metal dispersion diminishes the (de)hydrogenation function. On the other hand, an improvement in metal sulfidation may increase the (de)hydrogenation function. Since qantification of the two opposite effects is difficult, from these characterization results alone it is not clear what could be the net effect of F^- content on the (de)hydrogenation function. However, considering previous results (11) the following trends in catalytic activity were found: fluoride has almost effect or only a slightly positive one (depending on the reaction temperature) on the HDS of thiophene; a positive effect of the fluoride content on the pyridine HDN reaction has been disclosed, while a negative one has been found for butenes hydrogenation during the HDS of thiophene. The former facts suggest that (de)hydrogenation function increases with F^- content. More recent results of gas oil HDS at high pressure on the same catalysts have also shown that fluoride incorporation enhances the HDS activity considerably

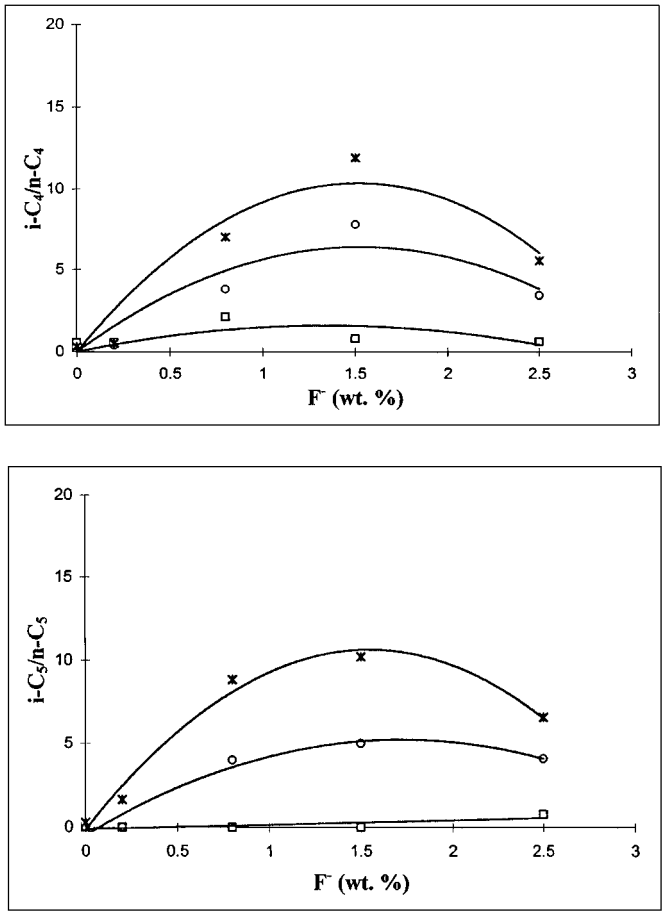

FIG. 7. Effect of fluoride content on the iso/normal butanes and pentanes molar ratio in the reaction products on NiW–F(x) catalysts at 673 K (□); 698 K (○), and 723 K (∗). W/F = 5 g · h · mol^{-1}.

(19). Collectively the above results look as if F^- increases the (de)hydrogenation function of the NiW catalysts. Concerning the acidic function, it was found that increasing F^- content slightly increased the number of acid sites but decreased the average acid strength (11, 20). Although the acid site density has been increased, as the acid strength has been diminished, we can consider that the balance is likely of weaker acidity, as the product selectivity suggests.

As a consequence of all this, the (de)hydrogenation function seems to be predominant over the acidity function at increasing fluoride content. This improvement in the balance between the (de)hydrogenation function and the acidity can explain that the overall conversion of *n*-heptane increases with increasing fluoride content, since a higher (de)hydrogenation function favor the formation of olefinic intermediates on metal sulfides, and by other hand that the rate of hydroisomerization increases relatively more than that of hydrocracking with increasing fluoride content because the acidity function is weaker. Note that cracking via carbonium and carbenium ions requires stronger acid sites while isomerization is catalyzed by less strong or medium acid sites (13, 23). The observed decrease in the strength of the acid sites may improve the balance of the acid-(de)hydrogenation functionalities and lead to a shift in the catalytic properties towards a more "ideal" hydroconversion of *n*-heptane on sulfided NiW–F(*x*) catalysts, as the evolution of product selectivity indicates.

The observation that C_7 isomers and hydrocracked products appear as primary reaction products, suggests that hydroisomerization and hydrocracking do not only take place as consecutive reactions (cracking following isomerization of *n*-heptane) but also as parallel reactions, although to a different extent depending on the catalyst. However, this does not mean that the hydrocracked products result from a direct β-scission of linear C_7 but that both reactions hydroisomerization and hydrocracking may proceed via a common reaction intermediate involving C_7^+ carbenium ions. The extremely low value of the *i*-C_4/*n*-C_4 ratio obtained with all the catalysts, and especially with the NiW–F(0) catalyst (about 0.05), contrasts with the expected value (>1) according to the theory of the classical cracking mechanism via carbenium ions (12, 14, 17, 22, 23). Note that under typical catalytic cracking conditions the iso/normal ratio in the butanes is generally high and above the thermodynamic equilibrium ratio (22–24). Moreover, on the NiW–F(*x*) catalysts the hydrocracked product distribution patterns were asymmetric, exhibiting notable amounts of C_5 and C_6 and, in some cases, also small amounts of C_1 and C_2 which can not be accounted for in the classical bifunctional cracking mechanism. All these features clearly indicate that, although with increasing F^- the behavior of the catalysts tends towards more "ideal" cracking behavior, in general the sulfided NiW–F(*x*) catalysts do not reach the "ideal" hydrocracking behavior observed for noble metals supported on zeolites (15, 25). In the latter bifunctional zeolitic catalysts the appearance of cracked products as primary reaction products occurs when the ratio of strong acid sites to metallic sites catalysts is high and, therefore, part of the olefinic intermediates during their migration find enough acid sites to crack before they are adsorbed and hydrogenated on the metallic sites (25). Apparently, this is the situation in the present fluoride-free and 0.2 wt% F^- containing NiW catalysts in which the (de)hydrogenation function of the nickel and tungsten sulfide phases is relatively weak compared to their acidity according to the hydroisomerization/hydrocracking selectivity obtained. As a result of the imbalance between the (de)hydrogenation and the acidic function of the NiW–F(0) catalyst, even at a conversion as low as 1%, the selectivity to hydrocracking was almost equal to that for hydroisomerization, suggesting a very high activity of the acid sites or the presence of very strong acid sites in the sulfided NiW–F(0) catalyst. With increasing fluoride content a better balance between the hydrogenation and the acidic function of the catalyst is reached and consequently the reaction selectivity changed towards higher hydroisomerization and lower hydrocracking (Fig. 1).

Examination of the relative distribution of the C_7 isomers, Fig. 5 shows that for the NiW–F(0) and NiW–F(0.2) catalysts the 3-MC_6/2-MC_6 molar ratio was about 1.5, which is not far of the value 2 predicted by the protonated cyclopropane (PCP) mechanism (26), indicating that the contribution of the PCP mechanism to branching of *n*-heptane is important over these catalysts, as it was also observed for sulfided NiMo/HY zeolites (6). The decrease in the 3-MC_6/2-MC_6 ratio from 1.5 to 1 with increasing fluoride content is most likely due to the relative slowdown of the cracking reaction, so that there is more time for a consecutive type A-rearrangement (27) of the 3-MC_6 carbenium ion to the 2-MC_6 one by the classical mechanism via hydride and alkyl shifts. It is not excluded, however, the possibility that the decrease of the 3-MC_6/2-MC_6 ratio with increasing fluoride content could be also due to a shift of the isomerization mechanism towards the classical one via alkyl-shifts, where a 3-MC_6/2-MC_6 ratio of 1 is predicted. The reason for this variation of the isomerization mechanism could be that the decrease in the average acid strength of the catalysts reduces the average lifetime of the chemisorbed carbocations, and this may favor a direct branching mechanism via alkyl shifts, leading to a relatively more abundant formation of 2-MC_6, although this isomerization route is energetically unfavorable for long chain paraffins. It is noteworthy, however, that the values of apparent activation energy for hydroisomerization obtained over the present work were relatively high and varied without a clear trend in the range 36–41 Kcal/mol. These values are very close to those reported for isomerization of *n*-heptane to 3-MC_6 (38.3 Kcal/mol) and to 2-MC_6 (41.3 Kcal/mol) over PtHY

zeolite catalysts (28). In this study the results of formation of 3-MC_6 and 2-MC_6 were better described by the classical mechanism through the 1,2-methyl shift than by the PCP mechanism. In the present work, possible changes in activation energy as a result of the shift of the isomerization mechanism cannot be observed. They are probably within the experimental error of the measurements.

The absence of multibranched C_7 isomers can be due to the sequential isomerization mechanism of *n*-heptane → monobranched C_7 → multibranched C_7, and to the lower rate of formation of multibranched isomers, or to the faster cracking rate of the dibranched isomers of *n*-heptane compared to the monobranched isomer (4). However, the last explanation seems unlikely, because if the main cracking route for the observed hydrocracked products is considered to be the β-scission of dibranched isomers, it should lead to an *i*-C_4/*n*-C_4 ratio $\geq$1 (4, 6), which is not observed in the results of Table 1, where *n*-butane (and not iso-butane) was predominantly obtained. This large amount of *n*-C_4 which appeared as a primary product, and in about equimolar amounts with propane for the NiW–F(0) catalysts, could be the result from type C of β-scission (29) of the methylhexane carbenium ions as shown.

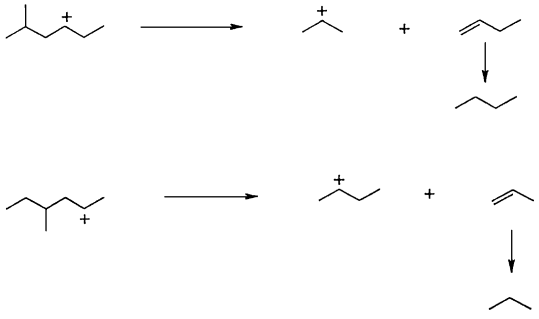

However, this is not the only mechanism able to give high *n*-C_4/*i*-C_4 ratios. Since in all cases substantial amounts of C_5 and C_6 appeared as primary products and C_1, and C_2 were mostly absent, only a very small part of the C_5 and C_6 production could arise from hydrogenolysis activity on the metal sulfides. The majority of the C_5 and C_6 may result from a dimerization or bimolecular reaction between heptenes and alkylcarbenium ions into C_{14} intermediates and the subsequent cracking through some of the reaction paths shown below which has been suggested in previous studies on *n*-heptane hydrocracking in bifunctional zeolite catalysts (4, 6, 17, 18, 21):

$$C_7^{=} + C_7^{+} \rightarrow [C_{14}^{+}] \rightarrow C_6 + [C_8^{+}] \rightarrow \cdots]$$

$$\searrow C_5 + [C_9^{+}] \rightarrow \cdots$$

$$\searrow C_4 + [C_{10}^{+}] \rightarrow \cdots$$

$$\searrow C_3 + [C_{11}^{+}] \rightarrow \cdots$$

This reaction scheme and the consecutive cracking of the $[C_8^+]$ to $[C_{11}^+]$ carbenium ions allow us to explain the abundant presence of C_5 and C_6 and also of C_3 and C_4. Also, it can generate abundant linear fragments, including *n*-butane (18). As deduced from the distribution of the hydrocracked products (Table 1), the relative contribution of the dimerization cracking mechanism remains important in the NiW–F(0) catalyst and becomes less important as the fluoride content is increased in the catalyst. This catalytic behavior of the NiW–F(0) catalyst is due to the insufficient balance between its (de)hydrogenation function and acidity, which appears with relatively lower acid site density but with higher acid strength compared to those with high F^- content. The occurrence of a bimolecular mechanism has also been found in different bifunctional catalysts with strong acidity insufficiently balanced by the (de)hydrogenation functionality of metal sulfides (6) or noble metals (18, 25). The observed increase in the *iso*/*n* ratios in the C_4 and C_5 fractions with increasing fluoride content (up to 1.5 wt% F) is also in line with a higher contribution of the classic bifunctional hydrocracking mechanism, i.e. that carbenium ions undergo isomerization prior to cracking. As shown by Fig. 7, this seems to be more important when the temperature is increased. It appears, however, that at 2.5 wt% F^- as the *i*-C_4/*n*-C_4 and *i*-C_5/*n*-C_5 ratios decrease, there is a minor contribution of the classic bifunctional hydrocraking. This can be attributed to a weakening of the acidic function of this catalyst, in which the increase in acid site density is counterbalanced by a lower strength of its acid sites, decreasing the ability for β-scission reactions since such reactions involve strong acid sites.

CONCLUSION

The results reported in this work show that sulfided alumina-supported NiW catalysts possess an equilibrated activity for hydroisomerization and hydrocracking of *n*-heptane. It is found that the incorporation of increasing amounts of fluoride to alumina-supported NiW catalysts shifts the catalyst behavior toward a more ideal bifunctional mechanism in the *n*-heptane transformation, improving the conversion of *n*-heptane and the selectivity to hydroisomerization with respect to cracking. The NiW sulfides supported on fluorided alumina can be promising in mild hydroprocessing oriented to enhance hydroisomerization.

ACKNOWLEDGMENTS

Financial support of this work by the DGICYT, Spain (Projects PB87-0261 and CE93-0012) is gratefully acknowledged. Two of the authors (A.L.A. and J.C.R.) are grateful to the Commission of the European Union for financial support (Project S/Cl*-913081) of J.C.R. in Spain. A. Benitez gratefully acknowledges the fellowship from the CONACyT, México. Thanks are also due to Mr. J. A. Ojeda for assistance in the figures preparation.

REFERENCES

1. Dufresne, P., Bigeard, P. H., and Billon, A., *Catal. Today* **1**, 367 (1987).
2. Maxwell, J. E., *Catal. Today* **1**, 385 (1987).
3. Frank, J. P., and Le Page, J. F., *Stud. Surf. Sci. Catal.* **7**, 792 (1981).
4. Vázquez, M. Y., Escardino, A., and Corma, A., *Ind. Eng. Chem. Res.* **26**, 1495 (1989).
5. Leglise, J., El Qotbi, M., Goupil, J. M., and Cornet, D., *Catal. Lett.* **10**, 103 (1991).
6. Leglise, J., El Qotbi, M., and Cornet, D., *Collect. Czech. Chem. Commun.* **57**, 882 (1992).
7. Baudon, A., Lemberton, Y. L., and Guisnet, M., *Catal. Lett.* **36**, 245 (1996).
8. Welters, W. J. J., van der Waerden, O. H., Zandbergen, H. W., de Beer, V. H. J., and van Santen, R. A., *Ind. Eng. Chem. Res.* **34**, 1156 (1995).
9. Welters, W. J. J., van der Waerden, O. H., de Beer, V. H. J., and van Santen, R. A., *Ind. Eng. Chem. Res.* **34**, 1166 (1995).
10. Moon, S. H., and Song, C. I., *Abstracts of the 13th North Amer. Meeting of the Catal. Soc., Pittsburg, 1993*, p. PB52.
11. Benitez, A., Ramírez, J., Fierro, J. L. G., and López Agudo, A., *Appl. Catal. A: General* **144**, 343 (1996).
12. Corma, A., López Agudo, A., Nebot, I., and Tomás, F., *J. Catal.* **77**, 159 (1982).
13. Corma, A., Monton, J. B., and Orchilles, A. V., *Ind. Eng. Chem. Proc. Res. Dev.* **23**, 404 (1984).
14. Corma, A., Fornés, V., and Melo, F., *Appl. Catal.* **61**, 175 (1990).
15. Martens, J. A., Jacobs, P. A., and Weitkamp, J., *Appl. Catal.* **20**, 239 (1986).
16. Bolton, A. P., and Bujalski, R. L., *J. Catal.* **23**, 331 (1971).
17. López Agudo, A., Asensio, A., and Corma, A., *J. Catal.* **69**, 274 (1981).
18. Blomsma, E., Martens, J. A., and Jacobs, P. A., *J. Catal.* **155**, 141 (1995).
19. Benitez, A., Ramirez, J., and López Agudo, A., to be published.
20. Benitez, A., Ph.D. thesis, Universidad Complutense, Madrid, 1992.
21. Pines, H., and Haag, W. O., *J. Am. Chem. Soc.* **82**, 2471 (1960).
22. Tiong Sie, S., *Ind. Eng. Chem. Res.* **31**, 1881 (1992).
23. Tiong Sie, S., *Ind. Eng. Chem. Res.* **32**, 397 (1993).
24. Ogata, E., Kamiya, Y., and Ohta, N., *J. Catal.* **29**, 296 (1973).
25. Guisnet, M., Alvárez, F., Gianneto, G., Chevalier, F., and Perot, G., *Catal. Today* **1**, 415 (1987).
26. Weitkamp, J., and Jacobs, P. A., *Prepr. Am. Chem. Soc. Div. Pet. Chem.* **26**, 9 (1981).
27. Weitkamp, J., *Ind. Eng. Chem. Prod. Res. Dev.* **21**, 550 (1982).
28. Sakai, T., Goto, M., Hatano, K., and Kato, M., *Bull. Chem. Soc. Jap.* **48**, 696 (1975).
29. Weitkamp, J., Jacobs, P. A., and Marten, J. A., *Appl. Catal.* **8**, 123 (1983).